Polymer Journal, Vol. 35, No. 6, pp 476—483 (2003)

Synthesis and Properties of Side-Chain Cholesteric Liquid Crystalline Elastomers Containing Tetra-Vinyl Crosslinking Units

Bao-Yan ZHANG,† Jian-She HU, Ying WANG, and Jian-Hua QIAN

Center for Molecular Science and Engineering, Northeastern University, Shenyang 110004, People's Republic of China

(Received December 3, 2002; Accepted April 2, 2003)

ABSTRACT: The synthesis of side-chain cholesteric liquid crystalline elastomers containing crosslinking agent pentaerythriol tetra-*p*-allyloxybenzoate (M-1) and mesogenic monomer 4-cholesteryl-4′-undecenyloyloxybenzoate (M-2) is presented by hydrosilication reaction. The chemical structures of the monomers and liquid crystalline networks were confirmed by Fourier transform infrared (FT-IR) and proton nuclear magnetic resonance (^{1}H NMR) spectroscopy. Mesomorphic properties and phase behavior were investigated by differential scanning calorimetry, polarizing optical microscopy, and X-ray diffraction measurements. The influence of crosslinking units on phase behavior was discussed. The networks containing less than 8 mol% of crosslinking units showed elasticity, reversible phase transition and cholesteric grandjean texture. The glass transition temperatures increased and clearing temperatures decreased with concentration of crosslinking units.

KEY WORDS Cholesteric Phase / Liquid Crystalline Elastomers / Grandjean Texture /

Today, material science is directed towards the development of multifunctional and oriented structure. One example of such supermolecular systems is liquid crystalline networks (LCNs). Recently, many studies have centred on LCNs with anisotropic properties,[1–10] and especially networks with cholesteric structure have attracted considerable interest due to outstanding properties for advanced applications such as flat-panel displays, non-linear optics, and organic lacquer.[11–16] The unique optical properties of cholesteric liquid crystalline are related to the helical supermolecular structure. According to density of crosslinking, two new classes of cholesteric LCNs emerge: highly crosslinked cholesteric liquid crystalline thermosets (ChLCTs); and lightly crosslinked cholesteric liquid crystalline elastomers (ChLCEs). In the last decade, ChLCTs have been extensively investigated because helical structure of cholesteric phase is permanently fixed and optical properties become temperature independent.[17–23] Contrary to ChLCTs, ChLCEs combine the basic features of elastomers with anisotropy of physical properties of cholesteric liquid crystalline. Therefore, ChLCEs not only hold entropic elasticity and macroscopically stable molecular orientation, but also show reversible phase transitions between mesophase and isotropic phase during heating and cooling cycles. Compared with conventional LCEs, ChLCEs show unusual piezoelectric properties besides electro-optical and mechanical properties due to deformation of helical structure. Recent theoretical and experimental studies have suggested that piezoelectricity can be obtained from ChLCEs.[24–26] ChLCEs have potential to act like a device that transforms mechanical signal into optical signal when stress is parallel to cholesteric helix.[25,27] Therefore, ChLCEs have been considered to be a candidate for making the piezoelectric device. However, to the best of our knowledge, research on ChLCEs are few reported.[24–28] Consequently, it will be both necessary and useful to prepare various kinds of side-chain ChLCEs to explore potential applications.

In this paper, the synthesis of side-chain ChLCEs containing 4-cholesteryl-4′-undecenyloyloxybenzoate as mesogenic units and pentaerythriol-tetra-*p*-allyloxybenzoate as crosslinking units is described. Phase behavior and mesomorphic properties of the monomers and polymers were investigated by differential scanning calorimetry (DSC), polarizing optical microscopy (POM), and X-ray diffraction measurement. The influence of concentration of crosslinking units on phase behavior was discussed. The elasticity and piezoelectricity of obtained ChLCEs are being studied.

EXPERIMENTAL

Materials

Polymethylhydrosiloxane (PMHS M_n = 700–800) was purchased from Jilin Chemical Industry Co. Undecylenic acid was purchased from Beijing Jinlong Chemical Reagent Co., Ltd. Cholesterol was purchased from Henan Xiayi Medical Co. Toluene used in the hydrosilication reaction was first refluxed over sodium and then distilled. All other solvents and reagents were purified by standard methods.

†To whom correspondence should be addressed (E-mail: baoyanzhang@hotmail.com).

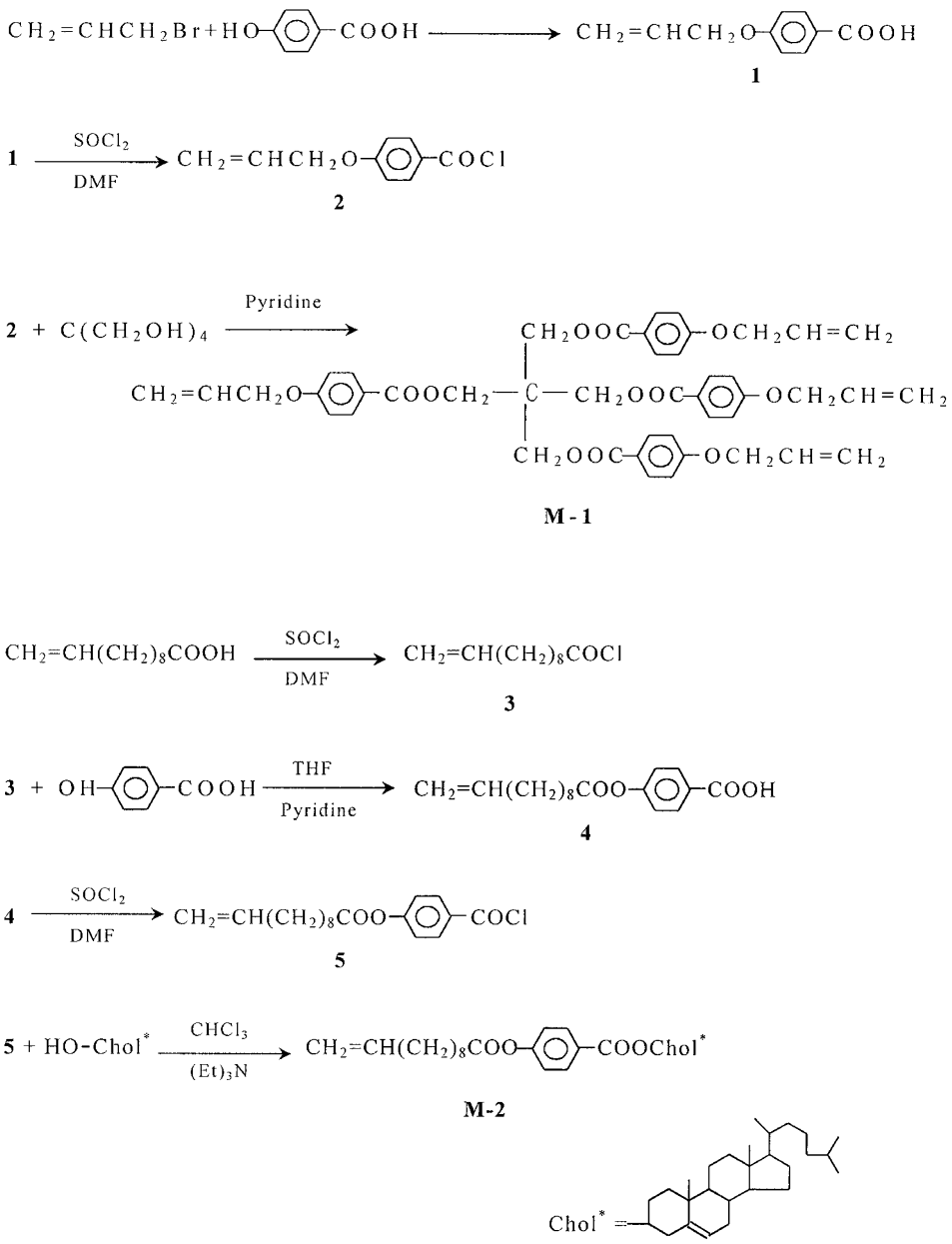

Scheme 1. Synthetic routes of monomers.

Characterization

^{1}H NMR spectra (300 MHz) were recorded on a Varian WH-90PFT spectrometer (Varian Associates, Palo Alto, CA). Fourier transform infrared (FT-IR) spectra were measured on a Nicolet 510 FT-IR spectrometer (Nicolet Instruments, Madison, WI, USA). Phase transition temperatures and thermodynamic parameters were determined using a PerkinElmer DSC-7 (PerkinElmer, Foster City, CA) equipped with a liquid nitrogen cooling system. Heating and cooling rates were 20 °C min^{-1}. Phase transition temperatures were taken during the second heating and first cooling scans. A Leitz Microphot-FX (Leitz, Wetzlar, Germany) polarizing optical microscope equipped with a Mettler FP 82 hot stage and FP 80 central processor were used to observe phase transition temperatures and analyze mesomorphic properties for liquid crystalline monomers and polymers through observation of optical texture. X-Ray diffraction measurements were performed with a nickel-filtered Cu-Kα radiation with a DMAX-3A Rigaku powder diffractometer.

Synthesis of Monomers

The synthetic route of vinyl monomers is shown in Scheme 1. 4-Allyloxybenzoic acid and 4-undecenyloyloxybenzoic acid were prepared according to the procedure as described by Hu.[29,30]

Pentaerythriol Tetra-p-allyloxybenzoate (M-1)

4-Allyloxybenzoyl chloride (39.4 g, 0.2 mol) was added dropwise to mixture of pentaerythrite (6.8 g, 0.05 mol) in dry pyridine (40 mL) at 0–5 °C. After

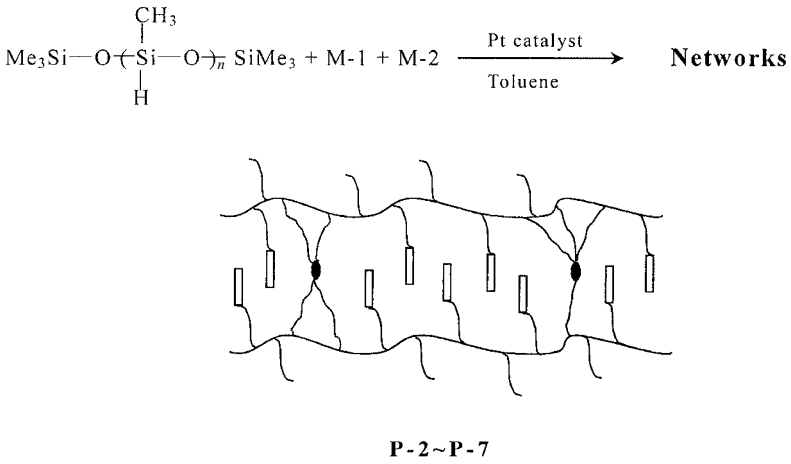

Scheme 2. Synthetic routes and schematic representation of polymer networks. (▭ mesogenic unit; ● crosslinking unit).

stirring for 5 h, the mixture was poured into cold water, precipitated, filtered and washed with water. The crude product was purified by recrystallization from ethanol. White crystals were obtained (mp = 83 °C, yield = 52%).

IR (KBr, cm^{-1}): 1720 (COO); 1633 (C=C); 1606, 1510 (Ar); 1255, 1164 (COC). ^{1}H NMR ($CDCl_3$, TMS) δ ppm: 4.35 (t, 2 H, –O–C$\underline{H}_2$–), 4.82–5.34 (m, 4 H, C$\underline{H}_2$= and –COO–C$\underline{H}_2$–), 5.97 (m, 1 H, =C$\underline{H}$–), 6.94–8.07 (m, 4 H, –$C_6\underline{H}_4$–).

4-Cholesteryl-4′-undecenyloyloxybenzoate (M-2)

4-Undecenyloyloxybenzoyl chloride (6.45 g, 0.02 mol) was added dropwise to a cold solution of cholesterol (7.74 g, 0.02 mol) in pyridine (1.6 mL) and chloroform (30 mL). The reaction mixture was stirred at 50 °C for 10 h. After removing precipitate by filtration, crude product was obtained by adding ethanol to filtrate, and recrystallized from toluene/ethanol (1 : 3). White solid were obtained (mp = 104 °C, yield = 46%).

IR (KBr, cm^{-1}): 1767, 1716 (COO); 1635 (C=C); 1603, 1504 (Ar). ^{1}H NMR ($CDCl_3$, TMS) δ ppm: 0.61–2.72 [m, 59 H, –(C$\underline{H}_2$)$_8$– and cholesteryl–H], 4.65–5.10 (m, 3 H, C$\underline{H}_2$= and –COO–C$\underline{H}$–), 5.50 (d, 1 H, =C$\underline{H}$– in cholesteryl), 6.08 (m, 1 H, =C$\underline{H}$–), 7.05–8.15 (m, 4 H, –$C_6\underline{H}_4$–).

Polymerization

The synthetic route of the polymers is performed in Scheme 2. For the synthesis of polymers P-1~P-7, the same method was adopted. The synthesis of polymer P-3 is given as an example.

Monomers M-1, M-2, and PMHS were dissolved in dry toluene. The reaction mixture was heated to 60°C under nitrogen, and then a proper amount of tetrahydrofuran solution of hexchloroplatinate hydrate catalyst was injected with a syringe. The reaction was kept for 24 h. The polymers were obtained by precipitation with excess methanol, washed with hot methanol, and then dried under vacuum.

IR (KBr, cm^{-1}): 1752, 1710 (C=O); 1608, 1505 (Ar); 1200–1000 (Si–O–Si).

RESULTS AND DISCUSSION

Synthesis

The synthetic routes for the target monomers and polymers are shown in Scheme 1 and 2. The structural characterization of the obtained monomers and polymers agreed well with the prediction. 4-Allyloxybenzoic acid **1** and 4-undecenyloyloxybenzoic acid **4** were synthesized according to a route described by Hu.[29,30] The crosslinking agent M-1 was prepared from pentaerythrite. Activation of **4** was obtained with thionyl chloride, then **5** was reacted with cholesterol in present of pyridine in chloroform to obtain cholesteric monomer M-2. The FT-IR spectra of monomers M-1 and M-2 showed characteristic bands at 1767, 1720, 1716 cm^{-1} due to ester C=O stretching, vinyl C=C absorption bands at around 1635 cm^{-1}, and aromatic at around 1606 and 1504 cm^{-1}. The ^{1}H NMR spectra of M-1 and M-2 showed multiplet at 8.15 to 6.94 ppm and 6.08 to 4.65 ppm, corresponding to aromatic and olefinic protons, respectively. In addition, M-2 exhibited a multiplet at 2.72 to 0.61 ppm due to methylene and methyl protons.

The polymer networks were prepared by hydrosilication reaction between Si–H groups of PMHS and vinyl C=C of cholesteric monomer M-2 and tetra-functional crosslinking agent M-1 in toluene, using hexchloroplatinate hydrate as catalyst at 60°C. Yields and detailed polymerization are listed in Table I. The obtained polymer networks were insoluble in toluene, xylene, *N*,*N*-dimethylformamide, chloroform etc., and were in

the form of rubber state. The FT-IR spectra of networks showed the complete disappearance of Si–H stretching band at 2160 cm^{-1} and vinyl C=C stretching band at around 1635 cm^{-1}. Characteristic absorption bands appeared at 1752 and 1710 cm^{-1}, 1608 and 1505 cm^{-1}, 1200–1000 cm^{-1}, corresponding to the stretching of ester C=O, aromatic, and Si–O–Si, respectively.

Thermal Properties

Thermal properties of the synthesized monomers and polymers were determined by DSC and POM. Phase transition temperatures and corresponding enthalpy changes are listed in Tables II and III, respectively. Typical DSC curves of M-2 and P-1~P-7 are shown in Figures 1 and 2.

Table I. Polymerization and yield

Polymer	Feed			M-1[a] (mol%)	Yields (%)
	PMHS (mmol)	M-1 (mmol)	M-2 (mmol)		
P-1	1	0.000	7.000	0	93
P-2	1	0.035	6.862	0.5	90
P-3	1	0.068	6.730	1.0	87
P-4	1	0.132	6.604	2.0	91
P-5	1	0.250	6.000	4.0	88
P-6	1	0.356	5.576	6.0	90
P-7	1	0.452	5.194	8.0	89

[a]Molar fraction of monomer M-1 based on M-1 + M-2.

DSC heating thermograms of M-2 showed a melting transition at 110.0 °C and liquid crystalline phase to isotropic transition at 195.5 °C. On cooling scans, an isotropic to liquid crystalline phase transition appeared at 185.5 °C as well as crystallization temperature at 69.4 °C. DSC thermograms of polymer networks P-1~P-6 containing various concentration of crosslinking units revealed glass transitions at low temperature and liquid crystalline phase to isotropic transitions at high temperature. Figure 3 shows the effect of the concentration of crosslinking units on phase transition temperature of polymer networks. It was clearly seen that low levels of crosslinking did not remarkably in-

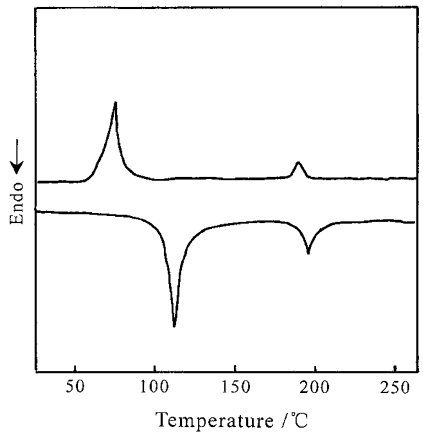

Figure 1. DSC thermograms of monomers M-2.

Table II. Thermal properties of monomers

Monomer	Phase transition temperature[a]/°C (Corresponding enthalpy changes/ J g^{-1}) Heating / Cooling	Yield (%)	ΔT^b
M-1	K83.6(50.16)I / I82.7(45.32)K	52	–
M-2	K110.0(20.64)Ch195.5(1.82)I / I185.5(0.54)Ch69.4(19.16)K	46	85.5

K = solid, Ch = cholesteric, I = isotropic. [a]Peak temperatures obtained by DSC were taken as phase transition temperature. [b]Mesomorphic temperature ranges.

Table III. DSC and POM for polymers

Polymers	DSC			ΔT^a	POM		$\lambda_m{}^d$/nm
	T_g /°C	T_i /°C	ΔH /J g^{-1}		$T_{cl}{}^b$ /°C	$T_{lc}{}^c$ /°C	
P-1	38.6	233.6	1.73	195.0	241	232	822
P-2	35.1	230.4	2.25	195.3	235	233	834
P-3	36.2	228.6	1.48	192.4	231	230	856
P-4	39.2	227.3	1.35	188.1	236	229	893
P-5	40.1	220.8	1.08	180.7	225	221	911
P-6	44.5	209.2	0.94	164.7	218	212	935
P-7	57.8	–	–	–	–	–	–

[a]Mesomorphic temperature ranges ($T_i - T_g$). [b]Temperature at which birefringence disappeared completely. [c]Temperature at which mesomorphic phase occurred. [d]Measured by UV-vis spectra at cholesteric phase.

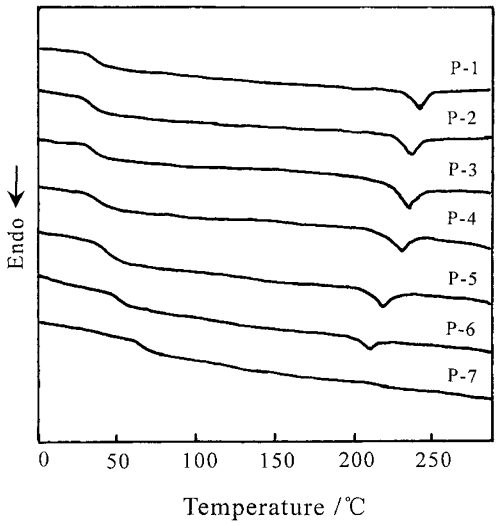

Figure 2. DSC thermograms of polymers.

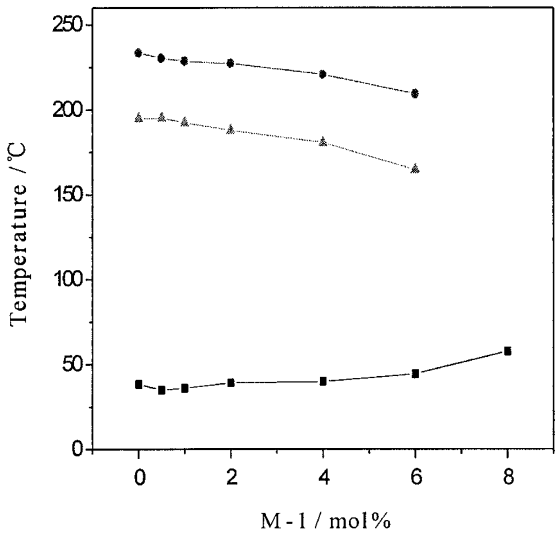

Figure 3. Effect of crosslinking concentration on phase transition temperatures of the polymers: ■ = T_g; ● = T_i; ▲ = ΔT.

fluence phase behavior, and reversible phase transitions were observed because of enough molecular motion and easy mesogenic orientation. In contrast, high levels of crosslinking had strongly influence on phase behavior, and could lead to liquid crystalline phase disappear due to less molecular motion and disturbance of liquid crystalline structure. Therefore, DSC curve of P-7 only showed a glass transition, no liquid crystalline phase to isotropic phase was observed. Above all phase transitions are reversible and do not change on repeated heating and cooling cycles, phase transition temperatures obtained in DSC are consistent with those observed by POM.

For side-chain ChLCEs, phase behavior and phase transition temperature depend on polymer backbone, rigidity of mesogenic unit, flexible spacer length, and crosslinking density. The backbones of side-chain ChLCEs are primarily polyacrylates, polymethacrylates, and polysiloxanes. However, polyacrylates and polymethacrylates, because of their backbones, show higher glass transition temperatures. To obtain mesomorphic properties at moderate temperature, polysiloxanes backbone, and flexible spacer are usually adopted. The polymer backbone and mesogenic units have antagonistic tendency, the polymer backbone is driven towards a random coil type configuration, while the mesogenic units stabilize with long range orientation order. The mesogenic units are usually attached to polymer backbone *via* a flexible spacer. The flexible spacer decouples the mesogenic side groups from polymer backbone and renders mesogenic units to order. Moreover, the polymers obtained by polymerizing cholesteric monomer can not only show smectic,[31–34] but also cholesteric[34–36] phase.

The glass transition temperature (T_g) is an important parameter in connection with structures and properties. In general, chemical crosslinking imposes additional constraints on the motion of chain segments, and makes T_g increase. However, the effect may be small for lightly crosslinked polymers. T_g can also be influenced by flexible crosslinking chains similar to the plasticization. Therefore, T_g of lightly crosslinked polymers may reduce compared with the precursor polymer. As seen from Figure 3, T_g of P-2 and P-3 was lower than that of precursor polymer P-1. However, general tendency is toward increased T_g with crosslinking density. For P-2~P-7, T_g increased from 35.1 to 57.8 °C when the concentration of crosslinking units increased from 0.5 to 8 mol%.

In addition, chemical crosslinking also affected liquid crystalline phase to isotropic phase transition. In general, nonmesogenic crosslinking units acted as diluent and was not in favour of the formation of mesogenic orientation in polymer networks. Consequently, the effect could lead to the clearing temperature (T_i) decrease with the concentration of crosslinking units. According to Table III and Figure 3, T_i of P-2~P-6 decreased from 230.4 and 209.2 °C when the concentration of crosslinking units increased from 0.5 to 6 mol%. Moreover, the enthalpy changes (ΔH) decreased from 2.25 to 0.94 J g^{-1}. For P-7 containing 8 mol% of crosslinking units, T_i was not observed due to less molecular motion and depression of mesogenic order. In addition, the mesomorphic temperature ranges (ΔT) of P-1~P-6 decreased from 195.0 to 164.7 °C because T_i decreased and T_g increased instead.

Optical Properties

The unique optical properties of cholesteric liquid crystalline are related to its helical supermolecular structure, the helical pitch of which controls the wave-

length of the selectively reflected light. Reflection color can be observed if pitch length is consistent with the wavelength of visible light. According to the Bragg equation:

$$\lambda_m = nP \cos \phi$$

the wavelength of the reflected light λ_m is related to the pitch P, average refractive n and incidence angle ϕ. When $\phi = 0°$ (normal incidence) $\lambda_m = \lambda_0 = nP$. The intensity of reflected light is a maximum at $\lambda_m = \lambda_0$, and it falls off very rapidly on either side of λ_0.[37]

The helical pitch is an important parameter in connection with structures and properties of cholesteric phase. Although the microscopic origins of pitch are still a subject of study, for side-chain cholesteric liquid crystalline polymers, it is known that the helical pitch and optical properties mainly depend on the polymer backbone, rigidity of mesogen, flexible spacer length, copolymer composition, molecular mass, and outer condition (such as temperature, force field, electric field, magnetic field etc). For each polymer, the maximum reflection wavelength λ_m was measured with UV-vis spectra. The λ_m-values are summarized in Table III. As can be seen from Table III, reflection color can not be observed because λ_m-value is greater than the wavelength of visible light. Moreover, with increasing the concentration of crosslinking units, λ_m-values increase, that is to say, P also increases.

The pitch affects not only selective reflection wavelength, but also optical texture of cholesteric phase. When the pitch lies within visible light, cholesteric phase exhibits planar oily streak or grandjean texture; when the pitch is much greater than wavelength of visible light, finger print texture can be observed; when the pitch less than the wavelength of visible light, focal conic texture is observed.

POM observation results showed that monomer M-2 exhibited enantiotropic cholesteric texture during heating and cooling cycles. However, no texture was observed for M-1. When M-2 was heated to about 104°C, the sample melt, cholesteric oily streak texture and reflection color appeared at 157°C. Reflection color changed from yellow and green to blue and violet with temperature, namely, pitch of cholesteric phase decreases and selective reflection of light shifts to the short wavelength region with increasing temperature. Cholesteric texture and reflection color disappeared at 202 °C. On cooling the sample from isotropic melt, focal conic texture was formed, which easily transformed to oily steak texture by shearing liquid crystalline phase. Reflection color disappeared and broken focal conic texture appeared at 152°C, and sample crystallized at 82 °C. Photomicrographs of M-2 are shown in Figures 4a and 4b.

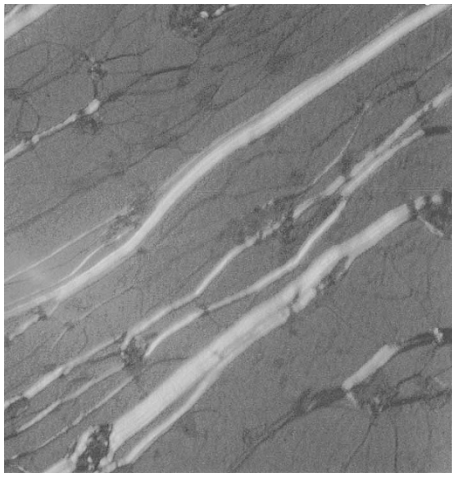

(a)

(b)

Figure 4. Optical polarizing micrographs of monomer M-2 (200×). (a) Oily streak texture at 167 °C. (b) Broken focal conic texture at 142 °C.

During heating and cooling cycles, the precursor polymer P-1 exhibited cholesteric grandjean and oily streak texture, the polymer networks P-2~P-6 exhibited cholesteric grandjean texture, P-7 showed only elasticity, and no mesomorphic property was observed, which is consistent with the results obtained by DSC. Therefore, liquid crystalline phase type and texture did not change when the concentration of crosslinking unit was less than 8 mol% for P-1~P-6. Photomicrographs of P-1 and P-4 are shown in Figures 5a and 5b as examples.

X-Ray Analysis

X-Ray studies are carried out to obtain more detailed information on liquid crystalline phase structure, especially smectic phase structure. In general, a sharp and strong speak at low angle ($1° < 2\theta < 4°$) appears in small-angle X-ray scattering (SAXS) curves only for smectic phase structure, and a broad peak associated with lateral packing at $2\theta = 18–21°$ is observed in wide-

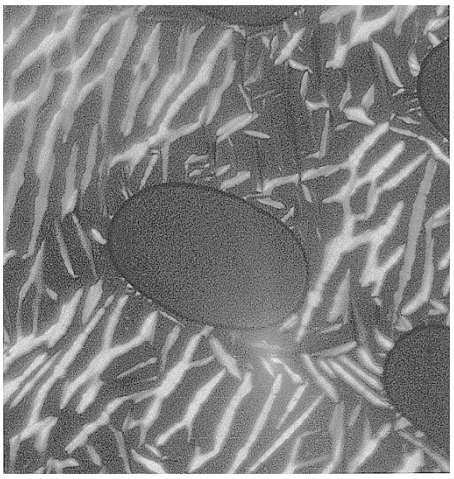

(a)

(b)

Figure 5. Optical polarizing micrographs of polymer (200×). (a) Oily streak texture of P-1 at 228 °C. (b) Grandjean texture of P-4 at 172 °C.

angle X-ray diffraction (WAXD) curves for nematic, smectic and cholesteric phase structures. For the polymers P-1~P-6, a sharp and strong speak at low angle did not appear in SAXS curves, which suggests that P-1~P-6 are not smectic liquid crystalline. Figure 6 only shows WAXD curves of quenched samples. Therefore, cholestreic phase structure of P-1~P-6 was confirmed by DSC, POM, and SAXS results. Moreover, broad peak was more diffuse and peak intensity reduced with increasing the concentration of crosslinking units in polymer networks, which indicates decrease of liquid crystalline order from P-2 to P-6. However, no sharp and broad peak was shown in SAXS and WAXD curve of P-7, which implies that P-7 has no mesomorphic property.

CONCLUSION

Side-chain cholesteric liquid crystalline elastomers containing both crosslinking agent M-1 and cholesteric monomer M-2 were synthesized. Lightly chemical

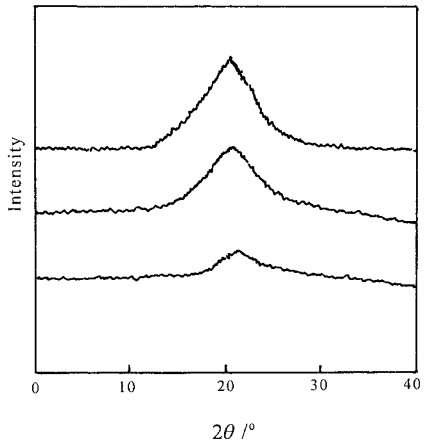

Figure 6. X-Ray diffraction pattern of quenched samples.

crosslinking of the linear polymer to elastomers did not markedly affect phase behavior. The polymer networks containing less than 8 mol% of crosslinking units revealed elasticity, reversible phase transition and cholesteric grandjean texture on heating and cooling cycles. For P-2~P-6, the glass transition temperatures increased, clearing temperatures and mesomorphic temperature ranges decreased with concentration of crosslinking units.

Acknowledgments. The authors are grateful to the National Natural Science Fundamental Committee of China and National Basic Research Priorities Programme (973) of China for financial support of this work.

REFERENCES

1. H. Finkelmann and G. Rehage, *Adv. Polym. Sci.*, **61**, 99 (1984).
2. D. J. Broer, J. Boven, and G. N. Mol, *Makromol. Chem.*, **190**, 2255 (1989).
3. M. Warner and X. J. Wang, *Macromolecules*, **24**, 4932 (1991).
4. K. Geibel, A. Hammerschmidt, and F. Strohmer, *Adv. Mater.*, **5**, 107 (1993).
5. S. Jahromi, J. Lub, and G. N. Mol, *Polymer*, **35**, 622 (1994).
6. M. Mauzac, H. T. Nguyen, F. G. Tournilhac, and S. V. Yablonsky, *Chem. Phys. Lett.*, **240**, 461 (1998).
7. M. Warner and E. M. Terentjev, *Prog. Polym. Sci.*, **21**, 853 (1996).
8. C. Ortiz, R. Rodighiero, C. K. Ober, and E. J. Kramer, *Macromolecules*, **31**, 4074 (1998).
9. C. S. Hsu and H. L. Chen, *J. Polym. Sci., Part A: Polym. Chem.*, **37**, 3929 (1999).
10. E. J. Choi, H. K. Ahn, J. K. Lee, and J. I. Jin, *Polymer*, **41**, 7617 (2000).
11. S. V. Belayev, M. I. Schadt, J. Funfschiling, N. V. Malimoneko, and K. Schmitt, *Jpn. J. Appl. Phys., Part 2*, **29**, L634 (1990).
12. D. J. Broer, J. Lub, and G. N. Mol, *Nature*, **378**, 467 (1995).
13. T. J. Bunning and F. H. Kreuzer, *Trends Polym. Sci.*, **3**, 318

(1995).
14. D. K. Yang, J. L. West, L. C. Chien, and J. W. Doane, *J. Appl. Phys.*, **76**, 1331 (1994).
15. P. M. Peter, *Nature*, **391**, 745 (1998).
16. B. Sapich, J. Stumpe, and H. R. Kricheldorf, *Macromolecules*, **31**, 1016 (1998).
17. D. J. Broer and I. Heynderickx, *Macromolecules*, **23**, 2474 (1990).
18. R. A. M. Hikmet, J. Lub, and D. J. Broer, *Adv. Mater.*, **3**, 393 (1991).
19. D. J. Broer, J. Lub, and G. N. Mol, *Macromolecules*, **26**, 1244 (1993).
20. J. Lub, D. J. Broer, R. A. M. Hikmet, and K. G. J. Nierop, *Liq. Cryst.*, **18**, 319 (1995).
21. H. R. Kricheldorf and T. Krawinkel, *Macromol. Chem. Phys.*, **199**, 783 (1998).
22. G. Maxein, S. Mayer, and R. Zentel, *Macromolecules*, **32**, 5747 (1999).
23. M. A. Espinosa, V. Cadiz, and M. Galia, *J. Polym. Sci. Part A: Polym. Chem.*, **39**, 2847 (2001).
24. R. Zentel, G. Reckert, S. Bualek, and H. Kapitza, *Makromol. Chem.*, **190**, 2869 (1989).
25. H. Brand, *Makromol. Chem., Rapid Commun.*, **10**, 441 (1989).
26. S. U. Vallerien, F. Kremer, F. W. Fischer, H. Kapitza, R. Zental, and H. Poths, *Makromol. Chem., Rapid Commun.*, **11**, 593 (1990).
27. M. Brehmer and R. Zentel, *Mol. Cryst. Liq. Cryst.*, **243**, 353 (1994).
28. S. M. Kelly, *J. Mater. Chem.*, **5**, 2047 (1995).
29. J.-S. Hu, B.-Y. Zhang, Z.-L. Feng, H.-G. Wang, and A.-J. Zhou, *J. Appl. Polym. Sci.*, **80**, 2335 (2001).
30. J.-S. Hu, B.-Y. Zhang, L.-M. Liu, and F.-B. Meng, *J. Appl. Polym. Sci.,* in press.
31. H. Finkelmann, H. Ringsdorf, W. Siol, and H. Wendorff, *Makromol. Chem.*, **179**, 829 (1978).
32. H. Finkelmann in "Polymer Liquid Crystals", A. Ciferri. Ed., Academic Press, New York, N.Y., 1982, p 35.
33. Q.-Z Zhang and Y. Wang, *Chem. J. Chinese Univ.*, **15**, 928 (1994).
34. E. Chiellini, G. Galli, C. Malanga, and N. Spassky, *Polym. Bull.*, **9**, 336 (1983).
35. J.-G. Zhi, B.-Y. Zhang, B.-L. Zang, and G.-H. Shi, *J. Appl. Polym. Sci.*, **85**, 2115 (2002).
36. J.-S. Hu, B.-Y. Zhang, Y.-G. Jia, and Y. Wang, *Polym. J.*, **35**, 160 (2003).
37. P. Das, J. Xu, and J. Roy, *J. Chem. Phys.*, **111**, 8240 (1999).